

Article

Cobalt-Substituted Seven-Layer Aurivillius $\text{Bi}_8\text{Fe}_4\text{Ti}_3\text{O}_{24}$ Ceramics: Enhanced Ferromagnetism and Ferroelectricity

Zhiwei Lei ^{1,6}, Tong Chen ¹, Weigu Li ¹, Min Liu ^{1,3,4,*}, Wen Ge ¹ and Yalin Lu ^{1,2,3,4,5,*}

¹ CAS Key Laboratory of Materials for Energy Conversion, Department of Materials Science and Engineering, University of Science and Technology of China, Hefei 230026, China; lzwei@mail.ustc.edu.cn (Z.L.); aqct@mail.ustc.edu.cn (T.C.); weiguli@utexas.edu (W.L.); gew1024@mail.ustc.edu.cn (W.G.)

² Hefei National Laboratory for Physical Sciences at the Microscale, University of Science and Technology of China, Hefei 230026, China

³ Synergetic Innovation Center of Quantum Information & Quantum Physics, University of Science and Technology of China, Hefei 230026, China

⁴ Hefei Physical Sciences and Technology Center, CAS Hefei Institutes of Physical Sciences, Hefei 230031, China

⁵ National Synchrotron Radiation Laboratory, University of Science and Technology of China, Hefei 230026, China

⁶ Patent Examination Cooperation Sichuan Center of the Patent Office, Chengdu 610213, China

* Correspondence: liumin1106@ustc.edu.cn (M.L.); yllu@ustc.edu.cn (Y.L.)

Academic Editor: Iwan Kityk

Received: 12 January 2017; Accepted: 1 March 2017; Published: 8 March 2017

Abstract: In this work, Aurivillius-phase $\text{Bi}_8\text{Fe}_{4-x}\text{Co}_x\text{Ti}_3\text{O}_{24}$ (7-BFCT, $0 \leq x \leq 0.4$) powders and ceramics were successfully prepared by the combination of citrate combustion and hot-press methods. X-ray diffraction (XRD) and high-resolution transmission electron microscopy (HRTEM) indicate a successful synthesis of the pure phase of the 7-BFCT ceramics, and all the samples showed a good seven-layer structure of the Aurivillius phase. Partial Fe substituted by Co was found to be effective to enhance both ferromagnetic and ferroelectric properties at room temperature, and the largest remnant magnetization ($2M_r$) of ~ 0.69 emu/g was revealed at the composition of $x = 0.4$. Zero field cooling and field cooling (ZFC-FC) magnetization measurement confirmed its magnetic transition occurring at a high temperature of ~ 750 K. Correspondingly, the enhanced ferroelectric properties of such Co-substituted ceramics were also investigated.

Keywords: Aurivillius; ceramics; multiferroic; hot press

1. Introduction

The family of Bi-containing Aurivillius oxides are known potentially as single-phase multiferroics and have attracted much attention due to their excellent abundance with fundamental physics (unusual dielectric, magnetoelectric (ME) and high ferroelectric (FE) phase transition temperatures) and great application potential as sensors, and in multi-state memory, energy harvesting, etc. [1–5]. Such compounds have the general formula of $\text{Bi}_4\text{Bi}_{n-3}\text{Fe}_{n-3}\text{Ti}_3\text{O}_{3n+3}$ (BFTO), which can be formed by inserting one or more perovskite layers of multiferroic BiFeO_3 (BFO) into the three-layered $(\text{Bi}_2\text{Ti}_3\text{O}_{10})^{2-}$ perovskite slabs of the parental $\text{Bi}_4\text{Ti}_3\text{O}_{12}$ (BTO) ferroelectrics, and here n denotes the number of intermediate perovskite-like layers within a full unit cell [6]. The FE and ferromagnetism (FM) of the resulting BFTO can be driven from Ti ions with unoccupied d orbitals and Fe ions with partially filled d orbitals, respectively. Furthermore, $(\text{Bi}_2\text{O}_2)^{2+}$ layers in $\text{Bi}_4\text{Ti}_3\text{O}_{12}$ can play the key role as both space-charge compensation and insulation, with an expectation to be able to further reduce the leakage and improve fatigue properties as well [7].

Researchers have already revealed the coupled FE and the unwanted antiferromagnetic (AFM) behaviors in such compounds with $n = 4$ (4-BFTO) [8–10], 5 (5-BFTO) [11–13], and 6 (6-BFTO) [14,15]. In 2009, with Co partially substituted for Fe, a new $\text{Bi}_5\text{Fe}_{0.5}\text{Co}_{0.5}\text{Ti}_3\text{O}_{15}$ (4-BFCT) ceramic was investigated for the first time, which was found able to present a significant coexistence of FE and FM well above room temperature. Its remanent magnetization ($2M_r$) was improved to 7.8 memu/g, due to a possible existence of superexchange among oxygen-connected Fe and Co ions and the realigned spin structures caused by the substitution [16]. Following this work of using the Co substitution strategy, most recent investigations on $\text{Bi}_6\text{FeCrTi}_3\text{O}_{18}$ [13], $\text{Bi}_6\text{Fe}_{2-x}\text{Co}_x\text{Ti}_3\text{O}_{18}$ [17] ($n = 5$) and $\text{Bi}_7\text{Fe}_{3-x}\text{Ni}_x\text{Ti}_3\text{O}_{21}$ [18] ($n = 6$) also revealed an enhanced FM performance at or above room temperature. Remarkably, Wang et al. reported a plausible intrinsic magnetoelectric (ME) coupling in a five-layered Aurivillius ceramic, $\text{SrBi}_5\text{Fe}_{0.5}\text{Co}_{0.5}\text{Ti}_4\text{O}_{18}$, even at a high temperature of 373 K, surpassing almost all single-phase multiferroic materials currently under investigation [19]. Furthermore, by a nanoscale structural modulation, such ME coupling may be further enhanced due to the appearance of a new analogous morphotropic transformation effect [20]. In addition, Chen et al. revealed the formation mechanism of $\text{Bi}_5\text{Fe}_{0.9}\text{Co}_{0.1}\text{Ti}_3\text{O}_{15}$ nanosheets [21]. Apparently in the layered structure, FM properties can also be affected by the structure of the fundamental building blocks (here mainly referring to the layer number) [22]. Thus, it is worth considering what will happen if similarly using this substitution strategy in such layer-structured oxides with even higher n numbers. In fact, B-site substitution in a seven-layer $\text{Bi}_8\text{Fe}_4\text{Ti}_3\text{O}_{24}$ (7-BFTO) has never been done before, and no room-temperature FM was found in this material. Only a few previous works can be found with focuses on synthesis, crystalline structure and magnetic property studies of pure 7-BFTO, and most of them suggested the material's AFM behavior at room temperature [23–25].

2. Results and Discussion

2.1. X-ray Diffraction

Figure 1 shows the X-ray diffraction spectra of such as-prepared 7-BFCT ceramics. Due to the lack of standard Joint Committee on Powder Diffraction standards (JCPDS) cards of 7-BFCT, the XRD patterns in Figure 1 are compared with standard PDF cards of four-layer, five-layer and six-layer Aurivillius compounds, i.e., $\text{Bi}_5\text{FeTi}_3\text{O}_{18}$ —PDF#38-1257, $\text{Bi}_6\text{Fe}_2\text{Ti}_3\text{O}_{18}$ —PDF#21-0101, and $\text{Bi}_7\text{Fe}_3\text{Ti}_3\text{O}_{21}$ —PDF#54-1044, all of which show similar XRD patterns. All the XRD patterns in Figure 1 can be indexed by an orthorhombic lattice with the space group of $F2mm$, and it was found that all the samples are pure Aurivillius phase with no apparent impurity phase appearances. The peak located at about 30.75° slightly shifts to a larger angle (Figure 1b) as the Co concentration increases, indicating the small structural distortion arising from the Co substitution.

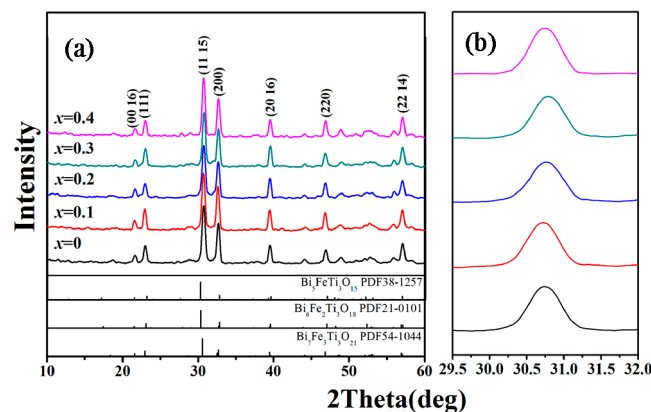


Figure 1. (a) X-ray diffraction spectra of the 7-BFCT ceramics and the standard PDF cards of $\text{Bi}_5\text{FeTi}_3\text{O}_{15}$, $\text{Bi}_6\text{Fe}_2\text{Ti}_3\text{O}_{18}$ and $\text{Bi}_7\text{Fe}_3\text{Ti}_3\text{O}_{21}$; (b) the enlarged spectra of the peak at about 30.75° .

2.2. High-Resolution Transmission Electron Microscopy

To verify the successful synthesis of 7-BFCT ceramics, Figure 2 shows the high-resolution transmission electron microscopy images of the 7-BFCT ceramics with various amounts of substituted Co. As shown in Figure 2, all samples had lattices consistent with several perovskite layers sandwiched by two $(\text{Bi}_2\text{O}_2)^{2+}$ layers. All samples showed a regular Aurivillius structure with $c/2$ around 3.2 nm, indicating the seven-layer structure [22] (Figure 2a–d). In addition, the lattice parameter c showed a slight decrease with the increase of x , suggesting the successful substitution of Co for Fe inside the lattices. When $x = 0.4$, although the sample was still a seven-layered structure, some stacking faults started to appear (Figure 2d), suggesting the maximum Co doping concentration in such materials before the secondary phase's appearance or the structural collapse caused by the too-large Co substitution.

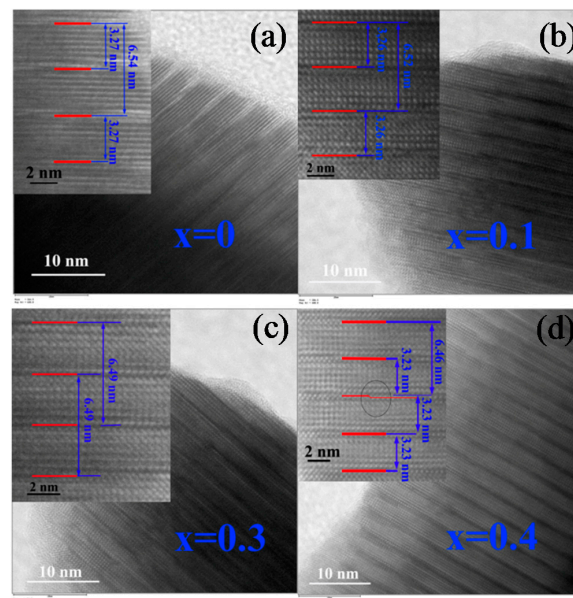


Figure 2. HRTEM images of the 7-BFCT ceramics with various Co substitution concentrations for Fe: (a) $x = 0$; (b) $x = 0.1$; (c) $x = 0.3$; and (d) $x = 0.4$.

2.3. Ferromagnetic Properties

Magnetic hysteresis loops of the 7-BFCT ceramics at room temperature and the corresponding zero field cooling and field cooling (ZFC-FC) magnetization measurements (the temperature dependence of M under a magnetic field of 500 Oe was recorded) were performed to visualize the ferromagnetic properties of the 7-BFCT, as presented in Figure 3. In Figure 3a, for the sample with $x = 0$ (the inset at the upper left of Figure 3a), the linear field dependence of the magnetization (M) indicates its AFM nature, similar to the results reported by Srinivas et al. [23]. The ZFC-FC magnetization measurements show that the undoped sample's Neel temperature (T_N), i.e., the antiferromagnetism-to-paramagnetism transition temperature, was ~ 247 K (Figure 3b), which further verifies the AFM nature of the pure 7-BFTO at room temperature. Noticeably, with the partial substitution of Co ions, magnetic hysteresis loops of the doped 7-BFCT ceramics ($x > 0$) all revealed the presence of the ferromagnetic moment (Figure 3a). Obviously, the FM properties of such seven-layered BFCT ceramics were significantly enhanced by the Co partial substitution, and $2Mr$ reached 0.04 emu/g, 0.30 emu/g, 0.35 emu/g and 0.69 emu/g for $x = 0.1, 0.2, 0.3$ and 0.4 samples, respectively. This enhancement could be explained by the possible superexchange among oxygen-connected Fe and Co ions, and the structure-modulated spin canting (the canting angle and the length between coupled ions) from the tilting of adjacent Fe–O and Co–O octahedrals [16–18]. Furthermore, Figure 3c reveals the ZFC-FC measurements of samples with $x = 0.1, 0.2, 0.3$ and 0.4 , and the curves indicate the magnetic Curie temperatures (here

also simplified as T_N) of such ceramics, the ferromagnetism-to-paramagnetism transition temperatures (marked as the peak of dM/dT curves), were about 776 K, 764 K, 762 K and 750 K, respectively, which are much higher than RT. It also shows a decreasing trend with the increase of the Co substitution concentration, and this can be attributed to the decreased orderliness of B-site ions and the relative stability of the magnetic structure by the increased Co substitution concentration [26]. Also, the ZFC and FC curves show that the spin glass transition temperatures of the 7-BFCT samples with $x = 0$ to 0.4 were about 247 K, 641 K, 633 K, 625 K and 623 K, respectively. This suggests that the substitution of Co for Fe may introduce some new magnetic exchange interactions which are worth investigating in the future. The detail values of $2M_r$ and T_N with different Co substitution concentrations are listed in Table 1. In order to recognize the ferromagnetic contribution from the magnetic impurities (e.g., CoFe_2O_4) or the BFCT host in Aurivillius ceramics [19,20], a derivative thermogravimetry (DTMG) measurement was performed in the nitrogen atmosphere at a heating rate of 20 K/min with a 200 Oe applied magnetic field on the sample $\text{Bi}_8\text{Fe}_{3.6}\text{Co}_{0.4}\text{Ti}_3\text{O}_{24}$ (7-BFCT-0.4). As shown in Figure 3d, there was a peak at 753.4 K in the derivative weight curve, corresponding to the T_N (750 K) measured using the ZFC-FC method, far higher than the 720 K of magnetic impurity CoFe_2O_4 [20]. Therefore, our 7-BFCT ceramics are ferromagnetic.

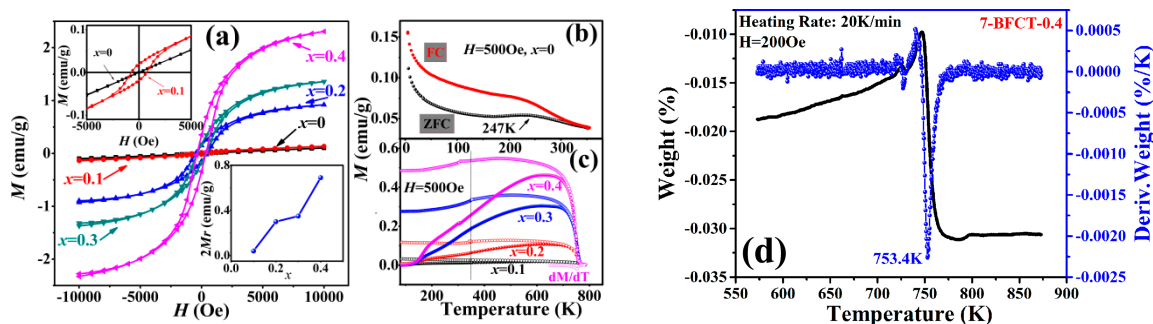


Figure 3. (a) M - H hysteresis loops of the 7-BFCT ceramics; and ZFC-FC measurements of the samples with (b) $x = 0$; and (c) $x = 0.1, 0.2, 0.3$ and 0.4 ; (d) weight loss and DTMG curves of 7-BFCT-0.4 ceramics.

2.4. Ferroelectric Properties

The room-temperature P - E hysteresis loops of the 7-BFCT samples under a driving field of 150 kV/cm are presented in Figure 4. As shown in Figure 4, the $2P_r$ of such 7-BFCT showed a great dependency on the Co substitution concentration. The $2P_r$ first increased with x and reached a maximum value of $4.15 \mu\text{C}/\text{cm}^2$ at $x = 0.3$, and then decreased as the concentration further increased. The increased polarization can be explained by the distortion of the crystalline structure by the Co substitution, as mentioned in the XRD analysis. The decreased of $2P_r$ at $x = 0.4$ could be attributed to the existing stacking faults, which may induce the destruction of the insulation of the $(\text{Bi}_2\text{O}_2)^{2+}$ layer. To rule out the possibility of artificial polarization from the leakage, a pulsed polarization positive-up-negative-down (PUND) measurement was performed and the results are shown in the inset of Figure 4. The measured switched polarization value (ΔP) was similar to the $2P_r$ obtained from the above hysteresis measurement, indicating the intrinsic ferroelectricity of the 7-BFCT samples.

In addition, to further realize the ferroelectricity of such 7-BFCT ceramics, the temperature dependence of the dielectric constant (ϵ) and the dielectric loss ($\text{Tan}\delta$) at 1 MHz were taken. Figure 5a shows the temperature dependence of the dielectric constant (ϵ) of the samples with $x = 0, 0.2$ and 0.4 . Their ϵ increases with the increase of the temperature and shows a dielectric peak at 1052 K, 1060 K and 1065 K for samples with $x = 0, 0.2$ and 0.4 , respectively. These temperatures are very close to the reported T_c , the ferro-paraelectric phase transition temperature, at ~ 1049 K [23]. The increased T_c can be explained by the substitution of smaller-radius ions (Co) for larger-radius ions (Fe), which would bring out a smaller tolerant factor and lead to the higher T_c . Figure 5b shows that the dielectric loss ($\text{Tan}\delta$) increases rapidly with increasing the temperature. Compared to the sample with $x = 0$,

the $\text{Tan}\delta$ values of the rest of the samples show a decrease and this may suggest a decreased defect concentration with the Co substitution [27]. The $x = 0.4$ sample shows a larger $\text{Tan}\delta$ than that of the sample with $x = 0.2$, and this could be explained by the increased defect concentration caused by the existing stacking faults, as suggested in both the HRTEM and ferroelectricity analyses before. Table 1 also lists the details of $2P_r$ and T_c of the samples with different x values.

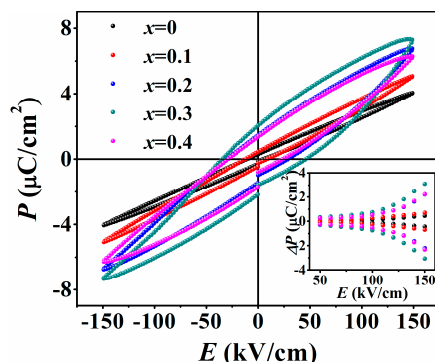


Figure 4. Room-temperature P - E hysteresis loops of the 7-BFCT samples under a driving field of 150 kV/cm (inset: plot of switched polarization vs. pulse amplitude for 7-BFCT samples from a PUND measurement).

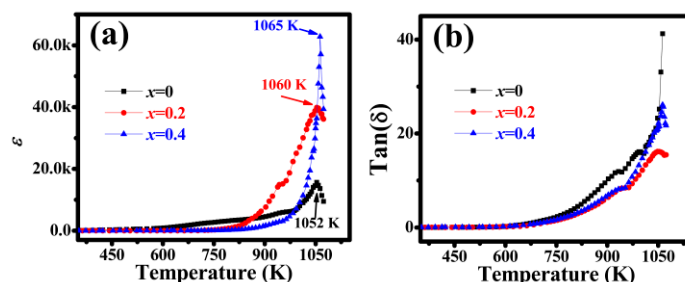


Figure 5. Temperature dependence of (a) dielectric constant (ϵ) and (b) dielectric loss ($\text{Tan}\delta$) at 1 MHz.

Table 1. The detail values of $2M_r$, $2P_r$, T_N and T_c with different Co substitution concentrations.

x	$2M_r$ (emu/g)	$2P_r$ ($\mu\text{C}/\text{cm}^2$)	T_N (K)	T_c (K)
0	–	0.59	247	1052
0.1	0.04	0.88	776	1054
0.2	0.30	2.90	764	1060
0.3	0.35	4.15	762	1062
0.4	0.69	3.05	750	1065

3. Materials and Methods

3.1. Sample Synthesis

Synthesis of the seven-layer $\text{Bi}_8\text{Fe}_{4-x}\text{Co}_x\text{Ti}_3\text{O}_{24}$ ($0 \leq x \leq 0.4$, 7-BFCT) powders and ceramics follows below procedures: stoichiometric amounts of $\text{Bi}(\text{NO}_3)_3 \cdot 5\text{H}_2\text{O}$ (99%), $\text{Fe}(\text{NO}_3)_3 \cdot 9\text{H}_2\text{O}$ (98.5%), $\text{Co}(\text{NO}_3)_3 \cdot 6\text{H}_2\text{O}$ (99%) and $\text{Ti}(\text{C}_{10}\text{H}_{16}\text{O})$ (tetrabutyl titanate, 98%) were firstly dissolved in the dilute nitric acid, then EDTA (ethylenediamine tetraacetic acid) and citric acid were added to form a stable colloidal solution. After dried, burned and heat-treated at 750 °C for 2 h, $\text{Bi}_8\text{Fe}_{4-x}\text{Co}_x\text{Ti}_3\text{O}_{24}$ powders were obtained. The corresponding ceramics were prepared by the hot-press method: firstly, the pre-sintered powders were pressed into pellets under a pressure of 80 MPa, then the pellet was placed in an alumina abrasive, and zirconium oxide powders were filled around the pellet as the isolation

layer. Finally, the pellets were sintered at 930 °C ($x = 0, 0.1$), 910 °C ($x = 0.2, 0.3$) and 900 °C ($x = 0.4$) for 3 h under a pressure of 10 MPa in the Ar/O₂ mixed atmosphere.

3.2. Characterization

Crystalline structures of the as-fabricated samples were investigated by X-ray diffraction (XRD, D/Max-gA, Toyko, Japan) with a Cu-K α radiation at $\lambda = 1.5405 \text{ \AA}$. Lattice images were taken by a high resolution transmission electron microscopy (HRTEM, JEM-2010, Japanese electronics co., LTD, Tokyo, Japan). Ferromagnetic properties were characterized using a vibrating samples magnetometer (VSM, EV-7, ADE Co., New York, NY, USA), and then the ferroelectric hysteresis loop was conducted using a Precision LC ferroelectric analyzer (Radiant Technology product, New York, NY, USA). Materials' dielectric properties were measured by an Agilent 4294A precision impedance analyzer. Derivative thermo-magneto-gravimetric (DTMG) measurements were realized by thermos-gravimetric analysis and application of a magnetic field of 200 Oe (TGA Q5000IR, New Castle, DE, USA).

4. Conclusions

In summary, Aurivillius Bi₈Fe_{4-x}Co_xTi₃O₂₄ (7-BFCT, $0 \leq x \leq 0.4$) powders and ceramics were successfully prepared by the combination of citrate combustion and hot-press methods. The effect of Co substitution on their ferromagnetic and ferroelectric properties was also investigated. All samples showed a good seven-layered structure with the largest remnant magnetization ($2M_r \sim 0.69 \text{ emu/g}$) obtained at $x = 0.4$, and the ferroelectric and magnetic transitions occurred at $\sim 1065 \text{ K}$ and $\sim 750 \text{ K}$, respectively. The sample with $x = 0.3$ revealed the largest $2P_r \sim 4.15 \text{ \mu C/cm}^2$ and $T_C \sim 1062 \text{ K}$. The superexchange between Fe-O-Co and the distorted crystal structure is responsible for the enhanced ferromagnetism. Changing of the ferroelectricity can be mainly attributed to the distorted crystalline structure and the existing stacking faults.

Acknowledgments: This work was supported by the Ministry of Science and Technology (2016YFA0400904), the External Cooperation Program of BIC, Chinese Academy of Sciences (211134KYSB20130017), the Key Research Program of Chinese Academy of Sciences (KGZD-EW-T06), the Hefei Science Center CAS (2015HSC-SRG052, 2015HSC-UE009, 2016HSC-IU004) and the State Key Laboratory of Solidification Processing in NWP (SKLSP201610).

Author Contributions: Min Liu and Zhiwei Lei conceived and designed the experiments; Zhiwei Lei and Weigu Li performed the experiments; Zhiwei Lei and Min Liu analyzed the data; Wen Ge contributed reagents/materials/analysis tools; Zhiwei Lei, Min Liu, Yalin Lu and Tong Chen wrote the paper.

Conflicts of Interest: The authors declare no conflict of interest.

References

1. Eerenstein, W.; Mathur, N.D.; Scott, J.F. Multiferroic and magnetoelectric materials. *Nature* **2006**, *442*, 759–765. [[CrossRef](#)] [[PubMed](#)]
2. Nan, C.W.; Bichurin, M.I.; Dong, S.; Viehland, D.; Srinivasan, G. Multiferroic magnetoelectric composites: Historical perspective, status, and future directions. *J. Appl. Phys.* **2008**, *103*, 031101. [[CrossRef](#)]
3. Suryanarayana, S.V.; Srinivas, A.; Singh, R.S. Magnetoelectric materials: Some recent results & possible applications. *Proc. SPIE* **1999**, *3903*, 232–265.
4. Diao, C.L.; Zheng, H.W.; Gu, Y.Z.; Zhang, W.F.; Fang, L. Structural and electrical properties of four-layers Aurivillius phase BaBi_{3.5}Nd_{0.5}Ti₄O₁₅ ceramics. *Ceram. Int.* **2014**, *40*, 5765–5769. [[CrossRef](#)]
5. Chen, X.Q.; Xiao, J.; Xue, Y.; Zeng, X.B.; Yang, F.J.; Su, P. Room temperature multiferroic properties of Ni-doped Aurivillius phase Bi₅Ti₃FeO₁₅. *Ceram. Int.* **2014**, *40*, 2635–2639. [[CrossRef](#)]
6. Lomanova, N.A.; Morozov, M.I.; Ugolkov, V.L.; Gusarov, V.V. Properties of Aurivillius phases in the Bi₄Ti₃O₁₂-BiFeO₃ system. *Inorg. Mater.* **2006**, *42*, 189–195. [[CrossRef](#)]
7. Lebeugle, D.; Colson, D.; Forget, A.; Viret, M.; Bonville, P.; Marucco, J.F.; Fusil, S. Room-temperature coexistence of large electric polarization and magnetic order in BiFeO₃ single crystals. *Phys. Rev. B* **2007**, *76*, 024116. [[CrossRef](#)]

8. Huang, F.Z.; Lu, X.M.; Chen, C.; Lin, W.W.; Chen, X.C.; Zhang, J.T.; Liu, Y.F.; Zhu, J.S. Room-temperature multiferroic properties of $\text{Bi}_{4.15}\text{Nd}_{0.85}\text{Ti}_3\text{FeO}_{15}$ thin films prepared by the metal-organic decomposition method. *Solid State Commun.* **2010**, *150*, 1646–1649. [[CrossRef](#)]
9. Ji, J.J.; Sun, H.; Mao, X.Y.; Wang, W.; Chen, X.B. Structure and multiferroic properties of $\text{Bi}_5\text{FeTi}_3\text{O}_{15}$ thin films prepared by the sol-gel method. *J. Sol-Gel Sci. Technol.* **2012**, *61*, 328–331. [[CrossRef](#)]
10. Li, J.B.; Huang, Y.P.; Rao, G.H.; Liu, G.Y.; Luo, J.; Chen, J.R.; Liang, J.K. Ferroelectric transition of Aurivillius compounds $\text{Bi}_5\text{Ti}_3\text{FeO}_{15}$ and $\text{Bi}_6\text{Ti}_3\text{Fe}_2\text{O}_{18}$. *Appl. Phys. Lett.* **2010**, *96*, 222903. [[CrossRef](#)]
11. Srinivas, A.; Suryanarayana, S.V.; Kumar, G.S.; Kumar, M.M. Magnetoelectric measurements on $\text{Bi}_5\text{FeTi}_3\text{O}_{15}$ and $\text{Bi}_6\text{Fe}_2\text{Ti}_3\text{O}_{18}$. *J. Phys.-Condens. Matter* **1999**, *11*, 3335–3340. [[CrossRef](#)]
12. Bai, W.; Xu, W.F.; Wu, J.; Zhu, J.Y.; Chen, G.; Yang, J.; Lin, T.; Meng, X.J.; Tang, X.D.; Chu, J.H. Investigations on electrical, magnetic and optical behaviors of five-layered Aurivillius $\text{Bi}_6\text{Ti}_3\text{Fe}_2\text{O}_{18}$ polycrystalline films. *Thin Solid Films* **2012**, *525*, 195–199. [[CrossRef](#)]
13. Yang, J.; Tong, W.; Liu, Z.; Zhu, X.B.; Dai, J.M.; Song, W.H.; Yang, Z.R.; Sun, Y.P. Structural, magnetic, and EPR studies of the Aurivillius phase $\text{Bi}_6\text{Fe}_2\text{Ti}_3\text{O}_{18}$ and $\text{Bi}_6\text{FeCrTi}_3\text{O}_{18}$. *Phys. Rev. B* **2012**, *86*, 104410. [[CrossRef](#)]
14. Bucko, M.M.; Polnar, J.; Lis, J.; Przewoznik, J.; Gaska, K.; Kapusta, C. Magnetic properties of the $\text{Bi}_7\text{Fe}_3\text{Ti}_3\text{O}_{21}$ Aurivillius phase doped with samarium. *Adv. Sci. Technol.* **2013**, *77*, 220–224. [[CrossRef](#)]
15. Kan, A.; Ogawa, H.; Inami, Y.; Moriyama, T. Synthesis and ferroelectric properties of bismuth layer-structured $(\text{Bi}_{7-x}\text{Sr}_x)(\text{Fe}_{3-x}\text{Ti}_{3+x})\text{O}_{21}$ solid solutions. *Phys. B Condens. Matter* **2011**, *406*, 3170–3174. [[CrossRef](#)]
16. Mao, X.; Wang, W.; Chen, X.; Lu, Y. Multiferroic properties of layer-structured $\text{Bi}_5\text{Fe}_{0.5}\text{Co}_{0.5}\text{Ti}_3\text{O}_{15}$ ceramics. *Appl. Phys. Lett.* **2009**, *95*, 082901. [[CrossRef](#)]
17. Liu, Z.; Yang, J.; Tang, X.W.; Yin, L.H.; Zhu, X.B.; Dai, J.M.; Sun, Y.P. Multiferroic properties of Aurivillius phase $\text{Bi}_6\text{Fe}_{2-x}\text{Co}_x\text{Ti}_3\text{O}_{18}$ thin films prepared by a chemical solution deposition route. *Appl. Phys. Lett.* **2012**, *101*, 122402. [[CrossRef](#)]
18. Sun, S.J.; Ling, Y.H.; Peng, R.R.; Liu, M.; Mao, X.Y.; Chen, X.B.; Knize, R.J.; Lu, Y.L. Synthesis of Ni-substituted $\text{Bi}_7\text{Fe}_3\text{Ti}_3\text{O}_{21}$ ceramics and their superior room temperature multiferroic properties. *RSC Adv.* **2013**, *3*, 18567–18572. [[CrossRef](#)]
19. Wang, J.L.; Fu, Z.P.; Peng, R.R.; Liu, M.; Sun, S.J.; Huang, H.L.; Li, L.; Knize, R.J.; Lu, Y.L. Low magnetic field response single-phase multiferroics under high temperature. *Mater. Horiz.* **2015**, *2*, 232–236. [[CrossRef](#)]
20. Sun, S.J.; Huang, Y.; Wang, G.P.; Wang, J.L.; Fu, Z.P.; Peng, R.R.; Knize, R.J.; Lu, Y.L. Nanoscale structural modulation and enhanced room-temperature multiferroic properties. *Nanoscale* **2014**, *6*, 13494–13500. [[CrossRef](#)] [[PubMed](#)]
21. Li, T.C.Z.A.; Chen, J.F.; Ge, W.; Liu, M.; Lu, Y.L. Hydrothermal synthesis and formation mechanism of Aurivillius $\text{Bi}_5\text{Fe}_{0.9}\text{Co}_{0.1}\text{Ti}_3\text{O}_{15}$ nanosheets. *CrystEngComm* **2016**, *18*, 7449–7456.
22. Jartych, E.; Mazurek, M.; Lisinska-Czekaj, A.; Czekaj, D. Hyperfine interactions in some Aurivillius $\text{Bi}_{m+1}\text{Ti}_3\text{Fe}_{m-3}\text{O}_{3m+3}$ compounds. *J. Magn. Magn. Mater.* **2010**, *322*, 51–55. [[CrossRef](#)]
23. Srinivas, A.; Kim, D.W.; Hong, K.S.; Suryanarayana, S.V. Study of magnetic and magnetoelectric measurements in bismuth iron titanate ceramic— $\text{Bi}_8\text{Fe}_4\text{Ti}_3\text{O}_{24}$. *Mater. Res. Bull.* **2004**, *39*, 55–61. [[CrossRef](#)]
24. Jartych, E.; Gaska, K.; Przewoznik, J.; Kapusta, C.; Lisinska-Czekaj, A.; Czekaj, D.; Surowiec, Z. Hyperfine interactions and irreversible magnetic behavior in multiferroic Aurivillius compounds. *Nukleonika* **2013**, *58*, 47–51.
25. Jartych, E.; Pikula, T.; Mazurek, M.; Lisinska-Czekaj, A.; Czekaj, D.; Gaska, K.; Przewoznik, J.; Kapusta, C.; Surowiec, Z. Antiferromagnetic spin glass-like behavior in sintered multiferroic Aurivillius $\text{Bi}_{m+1}\text{Ti}_3\text{Fe}_{m-3}\text{O}_{3m+3}$ compounds. *J. Magn. Magn. Mater.* **2013**, *342*, 27–34. [[CrossRef](#)]
26. Song, G.L.; Luo, Y.P.; Su, J.; Zhou, X.H.; Chang, F.G. Effects of Dy and Co co-substitution on the magnetic properties and T-C of BiFeO_3 ceramics. *Acta Phys. Sin.* **2013**, *62*, 097502.
27. Mao, X.Y.; Wang, W.; Sun, H.; Lu, Y.L.; Chen, X.B. Influence of different synthesizing steps on the multiferroic properties of $\text{Bi}_5\text{Fe}_1\text{Ti}_3\text{O}_{15}$ and $\text{Bi}_5\text{Fe}_{0.5}\text{Co}_{0.5}\text{Ti}_3\text{O}_{15}$ ceramics. *J. Mater. Sci.* **2012**, *47*, 2960. [[CrossRef](#)]

